Denervation atrophy of the head and neck muscles: MR appearances

Sayako Ohta, Mayumi Yasumoto, Hitoshi Shibuya
Department of Radiology Tokyo Medical and Dental University

Summery

Denervation atrophy can be detected as early as 15 days from the time of injury (8). The typical appearance of subacute denervation is high signal intensity distributed homogeneously throughout a denervated muscle on T2-weighted images (7, 8). In chronic stage, muscle volume decreases and fatty infiltration of the affected muscle becomes evident. MR imaging depicts denervation motor atrophy with excellent anatomy and contrast. Recognition of characteristic motor atrophy patterns helps to confirm clinically suspected nerve dysfunction and to facilitate determination of the site of nerve damage. It is also important to avoid confusing it with a primary neoplastic process.

Introduction

Cranial nerve dysfunction caused by tumors, infarction or inflammatory disorders results in motor neuron denervation atrophy of the head and neck muscles. The muscles in this area are often clinically inaccessible except for the facial muscles, and some are diminutive. CT evaluation of the characteristic muscular denervation atrophy patterns was reported previously (1). Although MR imaging enables to identify the muscles which cannot be distinguished by CT (2, 3), few MR images of denervation atrophy of the head and neck muscles have been demonstrated (4). Recognition of these atrophic patterns can provide an objective clue to clinically suspected cranial nerve deficits and prevent misinterpretation of their MR appearance.

We describe characteristic MR appearance of the muscular denervation atrophy of the head and neck with the exception of the facial muscles.

Imaging Techniques and Common Findings

Combination of spin-echo T1-weighted images and fast spin-echo T2-weighted images are basis of imaging head and neck muscles. Anatomy is generally well recognized on T1-weighted images. Normal muscles appear dark on both T1- and T2-weighted sequences, and fatty infiltration is detected as high signal intensity streak throughout the affected muscle on both sequences. If the muscle appears hyperintense to normal muscles only on T2-weighted images, it may suggest subacute denervation, reflecting increase of the extracellular water (7, 8). Short-tau inversion-recovery (STIR) is also reported to be the most sensitive technique in depicting the changes in denervated muscles during the subacute phase (8).

Motor innervation anatomy of the five cranial nerves is listed in **Table1**: V3, trigeminal nerve, mandibular division; IX, glossopharyngeal nerve; X, vagus nerve; XI, spinal accessory nerve; and XII, hypoglossal nerve (5, 6). Tensor tympani muscle was too minute to be visualized on routine MR imaging. The muscles of the infrahyoid neck were usually not included in the MR examinations to evaluate the five cranial nerve deficits.

Denervated muscles show muscle atrophy and fatty infiltration of the involved muscle group in the chronic stage of denervation (4, 7). MR imaging can identify most muscles of the head and neck and depict these changes in each muscle. Atrophy shows as asymmetrical volume loss of

Correspondence to : Dr. Sayako Ohta Department of Radiology Tokyo Medical and Dental University
1-5-45 Yushima, Bumkyo-ku, Tokyo JAPAN 113-8519
tel: 81-3-5803-5311 fax:81-3-5803-0147

Trigminal nerve mandibular division (V3)	Glossopharyngeal nerve (IX)	Vagus nerve (X)	Spinal accessory nerve (XI)	Hypoglossal nerve (XII)
Mm. of mastication tempolaris masseter pterygoids medial lateral Tensor tympani Tensor palati Mylohyoid Anterior belly of digastric	Stylopharyngeus	Mm. of soft palate * palatoglossus palatopharyngeus levator palati salpingopharyngeus Pharyngeal constrictors superior medial inferior (Cricothyroid) (Endolaryngeal Mm.)	Sternocleid-mastoid Trapezius	Mm. of tongue Intrinsic superior longituidinal inferior longituidinal vertical transverse Extrinsic genioglossus hyoglossus styloglossus Geniohyoid (Thyrohyoid) (Other strap muscles)

* Exculding the tensor palati muscle, Mm: muscles
Muscles in brackets are infrahyoid neck muscles.

Table 1 Approximate motor area supplied by the five cranial nerves

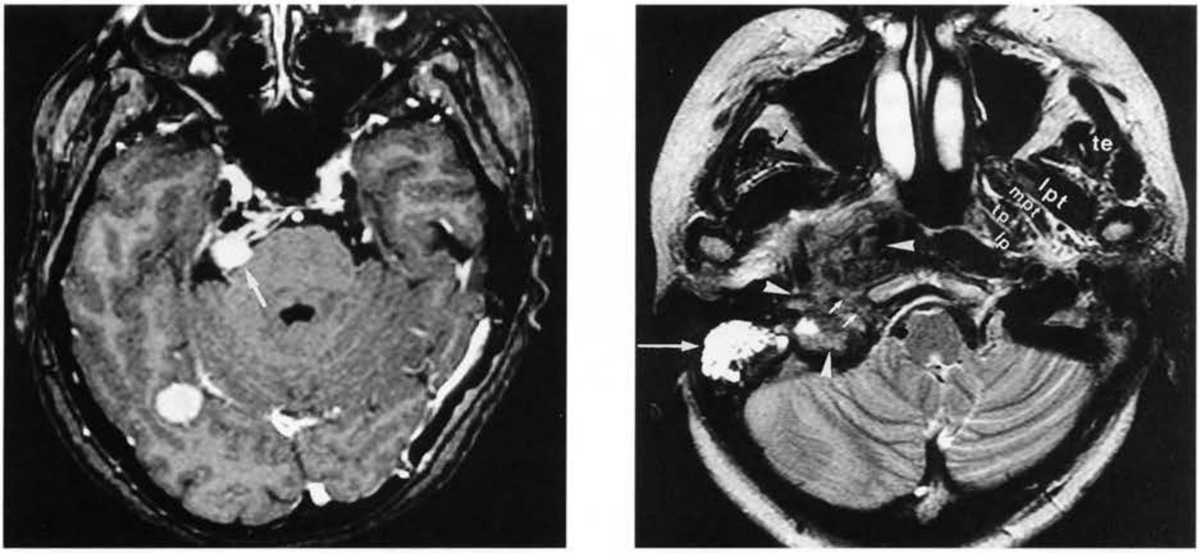

1-A 1-B

Fig1 42-year-old female with right trigeminal schwannoma and multiple menigiomas (right CP angle, jugular foramen, frontal falx, cerebellar hemisphere)

A, Axial gadolinium-enhance T1-weighted image shows schwannoma (white arrow) at the right trigeminal root and meningioma at the cerebellar tent.

B, Axial T2-weighted image at the level of nasopharynx shows meningioma (white arrowheads) in the right juglar foramen, extending into the parapharyngeal space and the hypoglossal canal (small white arrows). On the right side, the temporalis muscle (black arrow, V3) shows slight atrophic change, but the lateral pterygoid muscle (V3) shows no distinct atrophy. Note the right-sided otitis media (large white arrow) secondary to the tensor palati muscle dysfunction with the loss of normal eustachian tube function or compression by the tumor. Both changes reflect denerevation of the trigeminal nerve, mandibular division (V3). te = temporalis, lpt = lateral pterygoid, mpt = medial pterygoid, tp = tensor palati, lp = levator palati

1-C

C, Axial T2-weighted image at the level of upper oropharynx shows meningioma in the right parapharyngeal space. Atrophy and fatty change is detected in the masseter (black arrowhead, V3), stylopharyngeus (IX), pharyngeal constrictors (X), sternocleidmastoid (XI), styloglossus (XII), intrinsic tongue (white arrowheads, XII) on the right side. ma = masseter, sp = stylopharyngeus, p = pharyngeal constrictors, sg = styloglossus, it = internal tongue muscles

1-D

D, Axial T2-weighted image at the level of lower oropharynx shows atrophy of the mylohyoid (V3), sternocleidmastoid(XI), trapezius (XI), genioglossus (XII), styloglossus (XII), and hyoglossus (XII) muscles on the right. Posterior position of the tongue is also noted on the right side. mh = mylohyoid, scm = sternocleidmastoid, tr = trapezius, hg = hyoglossus, gg = genioglossus

2-A

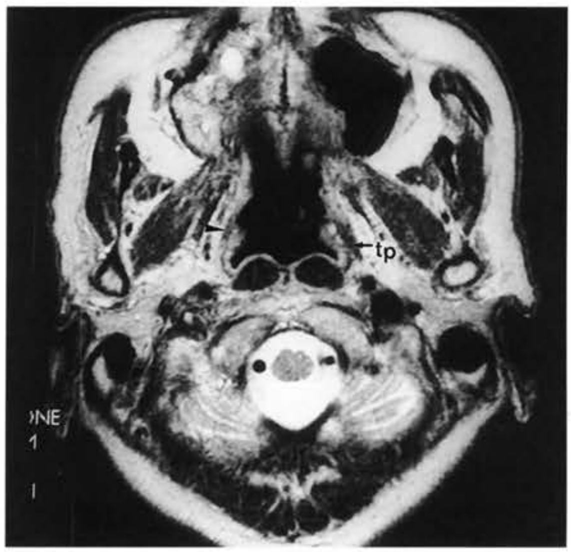

2-B

Fig. 2 60-year-old male with inflammatory granulomatous lesion in the right jugular foramen.

A, Axial T2-weighted image at the level of nasopharynx shows hyperintense granulomatous lesion in the right juglar foramen. The right levator palati muscle (black arrowhead, X) is almost completely atrophied behind the cartilagious part of the eustachian tube.

B, Axial T2-weighted image 3 mm lower level as A shows slight atrophic change of the right tensor palati muscle (black arrowhead, V3), probably due to disuse. No otitis media was recognized, suggesting patent eustachian tube function.

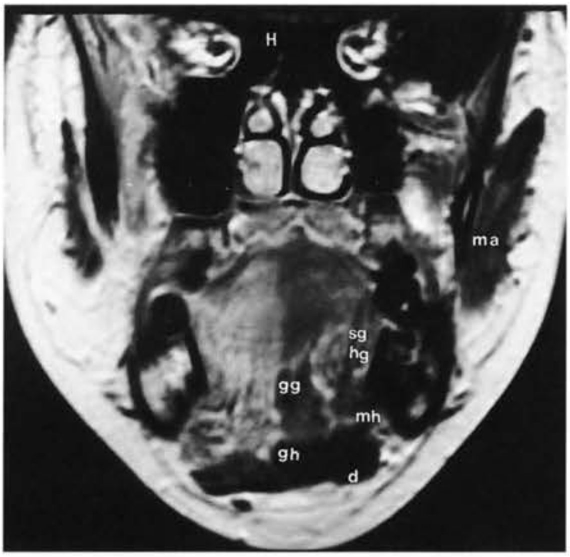

1-E

E, Coronal T1-weighted image shows atrophy and fatty change in the mylohyoid (V3), anterior belly of the digastric (V3), masster (V3), geniohyoid (XII), genioglossus (XII), styloglossus-hyoglossus (XII), and intrinsic tongue muscles (XII). gh = geniohyoid, d = anterior belly of digastric muscle

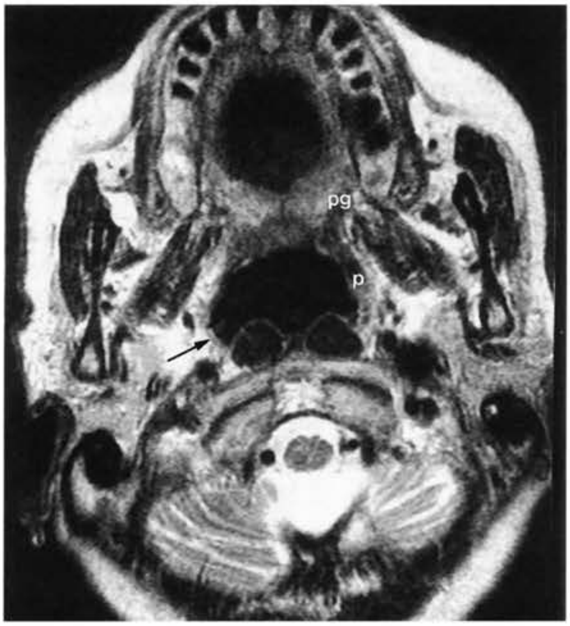

2-C

C, Axial T2-weighted image at the level of oropharynx shows marked atrophy of the pharyngeal constrictor (X), palatoglossus (X) muscles.

The pharyngeal cavity is unilaterally dilated (black arrow) on the right. pg = palatoglossus, p = pharyngeal constrictor

the affected muscles, and fatty infiltration results in increase of signal intensity of the muscle on both spin echo T1-weighted and fast spin echo T2-weighted sequences. Multiplanar imaging ability best demonstrates the distribution of these changes in the multiple muscles that are commonly innervated or in cases of multiple nerve deficits.

MR Appearance of Muscles of Each Affected Cranial Nerve

Mandibular division of the trigeminal nerve (V3)

Cell bodies of a motor root lie in the pontine part of the brainstem. The motor neurons to the muscles of mastication are the first to diverge from the main trunk of the mandibular nerve just after it exits the skull base. Nerve damage near or proximal to this first diverging point can result in denervation atrophy of all muscles innervated from the mandibular nerve: the muscles of mastication, tensor palati, tensor tympani, mylohyoid, and anterior belly of the digastric muscle **(Figs 1B-E, 3B)**. If nerve damage occurs distal to the first proximal motor branch, the four muscles of mastication can be spared from denervation atrophy. The second proximal motor branches supply the tensor tympani and tensor palati muscles. Besides atrophic change of tensor palati muscle, otitis media is seen as bright fluid signal in the mastoid on T2-weighted images, secondary to tensor palati muscle dysfunction with the loss of normal eustachian tube function **(Figs 1B, 3B)**.

Glossopharygeal nerve (IX)

Cell bodies of motor neurons of the glossopharyngeal nerve are located in the medulla. The glossopharyngeal nerve exits the jugular foramen in the anterior nasopharyngeal carotid space, curving round the lateral surface of the stylopharyngeus muscle to terminate in the posterior sublingual space. After the tympanic branch, the nerve supplies one motor innervation to the stylopharyngeus muscle. Its

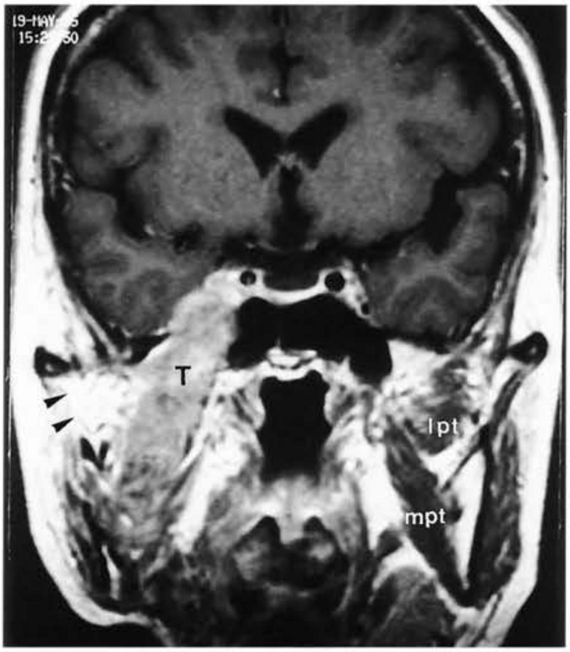

3-A

3-B

Fig.3 60-year-old female with recurrent adenoid cystic carcinoma in the right masticator space. The patient had the primary tumor in the right submandibular gland 13 years earlier.

A, Coronal gadolinium-enhanced T1-weight image shows recurrent tumor along the mandibular nerve in the right masticator space. Both medial and lateral (black arrowheads) pterygoid muscles show marked atrophy and fatty change. The masseter muscle also shows diffuse fatty infiltration. The right submandibular gland is excised. T = tumor

B, Axial T2-weighted image at the level of nasopharynx shows additional otitis media in the right mastoid (white arrow) caused by the atrophied tensor palati muscle. Diffuse fatty change of the muscles of mastication (V3) is also noted.

motor atrophy pattern is difficult to detect and it is possible only by MR imaging **(Fig 1C)**.

Vagus nerve (X)

Cell bodies of its motor neurons lie in the medulla. The nerve passes through the jugular foramen, joined by the cranial root of the accessory nerve (XI). They carry motor fibers to the muscles of the palate, pharynx, and larynx (except stylopharyngeus and tensor palati). Besides atrophy of the superior and middle pharyngeal constrictor muscles, unilateral dilatation of the pharyngeal cavity is seen on the affected side **(Figs 1C, 2C)**. Atrophy and fatty infiltration is also detected in the muscles of the soft palate. Both the levator palati and palatoglossus muscles can be routinely identified on MR images **(Figs 2A-C)**.

Spinal accessory nerve (XI)

The spinal root of the accessory nerve arises from cell bodies in the anterior horn of the cervical **(C2-4)** part of the spinal cord. Characteristic motor atrophy pattern of both sternocleidmastoid and trapezius muscles is easily recognized **(Figs 1D)**.

Hypoglossal nerve (XII)

Motor cell bodies of the hypoglossal nerve lie close to the midline of the caudal medulla. Although fatty change of intrinsic tongue muscles is recognized as a whole, atrophy or fatty infiltration of the individual extrinsic tongue muscles can be detected on MR imaging in various degrees **(Figs 1C-E)**. Posterior tongue position is also noted on the affected side, secondary to dysfunction of the extrinsic tongue muscles **(Fig 1D)**.

References

1. Harnsberger HR, Dillon WP. Major motor atrophic patterns in the face and neck: CT evaluation. Radiology 1985;155:665-670
2. Braun IF. MRI of the nasopharynx. Radiologic Clinics of North America 1989;27:315-330
3. Kassel EE, Keller MA, Kurcharczyk W. MRI of the floor of the mouth, tongue and oropharynx. Radiologic Clinics of North America 1989;27:331-351
4. Schellhas KP. MR imaging of muscle of mastication. AJR 1989;153:847-845
5. Anderson JE. Grant's atlas of anatomy. 7th ed. Baltimore: Williams & Wilkins, 1978, section 8
6. MacKinnon P, Morris J. Oxford textbook of functional anatomy volume 3 head and neck, Oxford: Oxford University Press, 1990, seminar 12, 14.
7. Fleckstein JL, Watumull D, Conner KE, et al. Denervated human skeletal muscle: MR imaging evaulation. Radioligy 1993;187:213-218
8. Uetani M, Hayashi K, Matsunaga N, Imamura K, Ito N. Denervated skeletal muscle: MR imaging. Radioligy 1993;189:511-515